JOURNAL OF CATALYSIS 155, 171–183 (1995)

The Influence of Support on the Activity of Monolayer Vanadia–Titania Catalysts for Selective Catalytic Reduction of NO with Ammonia

V. I. Marshneva, E. M. Slavinskaya, O. V. Kalinkina, G. V. Odegova, E. M. Moroz, G. V. Lavrova, and A. N. Salanov

Institute of Catalysis, Prosp. Akad. Lavrentieva 5, Novosibirsk 630090, Russia

Received May 9, 1995; revised March 6, 1995

An investigation of the influence of support on the activity of monolayer vanadia–titania catalysts in selective catalytic reduction (SCR) of NO by ammonia has been carried out. The V_2O_5–TiO_2 catalysts were prepared via $VOCl_3$ grafting on the TiO_2 surface, V_2O_5–WO_3–TiO_2 catalysts were prepared by inserting ammonium salts in TiO_2. The supports and catalysts were characterized by XPS, XRD, EPR, SIMS, electric conductivity, DRS UV–vis, BET, ICP, and X-ray fluorescence methods. The catalytic activity of samples was determined in a flow recycle reactor. On the basis of catalytic activity data it may be concluded that the specific activity, activation energy, and turnover frequency do not depend on the crystal structure of titania. The activation energy of the SCR process coincides with the vanadia reoxidation activation energy. Reoxidation of reduced vanadia species seems to be the rate-limiting step of the SCR process. NO SCR by ammonia with and without oxygen may have a common reaction mechanism. Conversion of one NO(NH_3) molecule proceeds on two surface vanadium atoms. Part of the supported vanadia penetrates into the sublayers of titania independent of the vanadia introduction method and titania crystal structure. © 1995 Academic Press, Inc.

1. INTRODUCTION

Selective catalytic reduction (SCR) of NO_x to nitrogen and water with ammonia has become an established technique for the removal of nitrogen oxides. In spite of numerous recent publications devoted to the mechanism and kinetics of SCR process on various V_2O_5–TiO_2 catalysts, there is as yet no common understanding of these problems. Thus, the available works present certain arguments concerning structure sensitivity (1) and insensitivity (2), realization of the SCR process via various intermediates (3, 4), various stoichiometry of reaction in the presence of oxygen (5), NO participation in NH_3 formation during the reaction (6), various values of activation energy (7, 8), and different monolayer concentrations of vanadium atoms (9–12).

The main reason for such a discrepancy may be the complexity of the process; the necessary simultaneous utilization of two oxidants, NO and O_2; the shortcomings of total gas analysis of reagents and products; the overwhelming number of experiments, performed with more or less significant diffusive effects (7, 13); and the frequent application of impregnated V_2O_5–TiO_2 catalysts containing various vanadium species and bulk V_2O_5 (14).

In particular, unlike the supported MoO_3–TiO_2 catalysts, for which the synthesis method is not critical, the amount of crystalline V_2O_5 in supported V_2O_5–TiO_2 can depend on the preparation procedure due to the lower surface diffusion rate for V_2O_5 (11).

Temperature-programmed desorption (TPD) studies on the model V_2O_5, V_2O_5–TiO_2, and TiO_2 (rutile) catalysts under ultrahigh vacuum, recently performed by Srnak *et al.* (8), revealed two adsorbed forms of ammonia with the desorption activation energies of 12–14 kcal/mol for the weak adsorbed ammonia species and 24–27 kcal/mol for the strong adsorbed ammonia species, in agreement with IR spectra investigations. The strong and weak adsorbed species of ammonia are related (20).

The well-known mechanism of NO–NH_3–O_2 (SCR) reaction on vanadia, proposed by Miyamoto *et al.* (15),

$$V{=}O + V_s{-}OH + NH_3 \rightarrow V{=}O \ldots NH_4 \ldots O{-}V_s \quad [1]$$

$$V{=}O \ldots NH_4 \ldots O{-}V_s + NO \rightarrow [\text{activated complex}]^* \quad [2]$$

$$[\text{activated complex}]^* \rightarrow V{-}OH + N_2 + H_2O + V_sOH \quad [3]$$

$$4\ V{-}OH + O_2 \rightarrow 2\ H_2O + 4\ V{=}O, \quad [4]$$

includes a number of essential features of the process, such as the role of V=O and V–OH surface species and the participation of both NH_3 and NO nitrogen atoms in the formation of N_2 molecules, as demonstrated by means of ^{15}N tracer studies.

Interaction of NO with NH_4^+ surface species agreed

0021-9517/95 $12.00

with the observation of the dominant role of Brønsted acid sites on the surface of V_2O_5. The reoxidation of V–OH groups by the lattice oxygen from the underlying layers was taken into account in the work of Miyamoto *et al.* (16). A similar point of view concerning the role of ammonium species was expressed by Topsøe (17) and Dines *et al.* (4) in their recent infrared spectroscopy studies of NO–NH_3 interaction on titania-supported vanadia catalysts.

An alternative mechanism, proposed by Janssen *et al.* (18), includes the dissociative adsorption of ammonia on the Lewis acid sites, more numerous on the surface of titania and titania-supported vanadia than on the surface of unsupported vanadia:

$$2\,V{=}O + NH_3 \rightarrow V{-}OH + V{-}ONH_2$$

$$V{-}ONH_2 + NO \rightarrow V{=}O + N_2 + H_2O$$

$$2\,V{-}OH \rightarrow V{=}O + V_{\blacksquare} + H_2O$$

$$2\,V_{\blacksquare} + O_2 \rightarrow 2\,V{=}O.$$

The reaction of gaseous NO and amidic species $-ONH_2$ agrees with the Farber and Harris observation of nitrosamide NH_2NO as an intermediate in the *in situ* mass spectrometric experiment (19). The recent IR spectroscopy studies of Dines *et al.* (4) revealed a band at 1332 cm^{-1}, tentatively assigned to another intermediate, V–O–N=N.

The competitive process, which can proceed on vanadia along with the SCR process, is the selective catalytic oxidation (SCO) of ammonia with oxygen. The accepted mechanism of NH_3 oxidation presumes that ammonia is split into NH_2 and H on the oxide anions with the fast reoxidation of metal ions (21). The same strong adsorbed NH_3 species are adopted in the mechanism of SCR, as proposed by Janssen *et al.* (18). At the low temperature of SCR process, 473 K, as was shown by Bjorklund *et al.* (22), the mechanism, involving V^{5+}–ONH_4 species, can be accepted. The application of V_2O_5 catalysts with different crystal morphology in the SCR of NO (23) has shown that V=O sites favor the direct oxidation of NH_3 and N_2O formation, while V–O–V sites give N_2.

The acceleration of the NO–NH_3 reaction by gaseous oxygen up to 1 vol% is well known (24). The surface oxygen of highly oxidized vanadia was shown to play the same role (25). The kinetic studies of NO–NH_3–O_2 reaction are often aggravated by the diffusion and give different specific activities, reaction orders, and activation energies (24). Inomata (26) has found for NO–NH_3 reaction the activation energy (E_a) to be equal to 16.7 kcal/mol, while in the presence of 1.3% oxygen it is only 11.7 kcal/mol with almost the same preexponential factor. Odenbrand *et al.* (27) obtained the very high value of E_a 45 kcal/mol under similar conditions.

Anatase is known as the best support for vanadia in the SCR reaction (1). Vejux and Courtine (28) explain the high activity of anatase-supported vanadia by the fitness of the (010) V_2O_5 plane and (001) anatase plane structures. Exposure of (010) plane leads to the increase of surface V=O groups concentration, thus providing a higher activity of monolayer vanadia–titania catalysts.

The influence of crystal structure of the TiO_2 support was investigated by Wong and Nobe (13). Above 473 K the specific activity of anatase-supported catalysts was higher than that of rutile-supported samples. E_a for the anatase-supported vanadia ranged from 13 to 10 kcal/mol with the method of vanadia introduction. The activation energy for the rutile-supported vanadia was 6.5 kcal/mol. Strong internal mass transfer effects were observed for all anatase supports. According to (29), rutile phase is a better support in NO reduction than anatase.

The approach of the present paper is to use the combination of the contemporary method of the monolayer catalyst preparation (30) with the physical methods of analysis and flow circulating kinetic method in order to obtain a new information about kinetic characteristics and specific activities within the vanadia monolayer and in order to understand both the role of TiO_2 crystal structure and the influence of such additives as Ti^{3+} and W^{6+} on the catalytic activity of the V_2O_5–TiO_2 system.

2. EXPERIMENTAL

2.1. Catalysts

Two modifications of TiO_2, designated further as A (anatase) and R (rutile) and marked by indices III, if prepared from a Ti^{3+} compound, or IV, if prepared from a Ti^{4+} were used as catalyst supports. The number in the catalyst designation (see, e.g., Table 1) stands for vanadia weight loading in wt%. Support AIV was prepared via hydrolysis of $TiCl_4$ solution in concentrated HCl under the action of 25 wt% ammonia solution at 343 K and pH 5–6. The resulting slurry was washed with deionized water to remove Cl ions and then dried for 2 h at room temperature and 10 h at 383 K and calcined for 6 h at 623 K. The support R IV was prepared by plasma treatment of $TiCl_4$.

Supports A III and R III were prepared via hydrolysis of $TiCl_3$ solution in HCl (1 : 1) under the action of NH_4OH solution at 273 K and pH < 6–7 for R III and pH > 7 for A III. The thermal treatment was performed similarly to that of A IV. The color of R IV and A IV was white. All other supports were yellowish and changed their color to white only after annealing at 1080 K.

TiO_2 samples were characterized by XPS, XRD, EPR, SIMS, electric conductivity, and DRS UV–vis methods. Chemical composition of the surface layers was analyzed using XPS on ESCA-spectrometer with two (AlK_α and

ZrM_ξ) types of radiation at E = 1486.6 and 151.4 eV, respectively. XPS spectra revealed oxygen and Ti^{4+} photoelectron lines with a C 1*S* line as impurity. The lines of Cl^- and Ti^{3+} ions were absent within the limits of method sensitivity (5% of monolayer). The X-ray fluorescence method has not revealed chlorine in catalysts or supports. The lack of alkaline metal impurities ($<10^{-3}$%) was confirmed by SIMS. The UV–vis diffusive reflection spectra of powdered TiO_2 supports were measured in the region of 45,000–11,000 cm^{-1}, using a Specord M 40 spectrometer.

The series of V_2O_5–TiO_2 catalysts were prepared via $VOCl_3$ grafting from the gas phase onto the TiO_2 surface, as described in (30). The samples of 0.5 g TiO_2 were successively treated for 2 h at 323 K with wet air (30% H_2O), 4 h at 413 K with dry air, and 14 h at 293 K with vapors of $VOCl_3$ in air and then slowly heated in a dry air flow to 623 K. The weight loading of vanadia depended on the number of treatment cycles. The prepared catalysts were calcined at 623 K in the flow of 10 vol% O_2 in He. The quantity of vanadium was determined by inductively coupled plasma (ICP) atomic emission spectrometry after the sample dissolved completely. The BET surface areas and vanadium atom surface concentrations are shown in Table 1.

The unsupported vanadia was of the extra pure grade and was prepared by thermal decomposition of NH_4VO_3 in oxygen. The unsupported tungsta was prepared by thermal decomposition of commercial extra pure ammonium *para*-tungstate in oxygen at 873 K for 10 h. The sample of commercial catalyst BASF-0481 for SCR was supplied by the BASF with permission to publish the kinetic data obtained. The vanadia–tungsta–titania catalysts (V–W–Ti) were obtained by inserting ammonium salts in TiO_2 at the different steps of preparation and annealing in oxygen at 823 K. The supported 1 wt% WO_3 was prepared via A IV impregnation with ammonium *para*-tungstate followed by drying at 383 K and annealing at 623 K.

The microphotographs of A III and R III samples were obtained with a BS-350 scanning electron microscope (Tesla, Czechoslovakia). Transmission electron microscopy was performed using a JEM-4000 EX to determine the structure of nanometer-sized particles of rutile R III. X-ray characteristics of supports and catalysts were obtained from diffractograms, recorded by HZG-4C apparatus (Freiberger Praezisionsmechanik GmbH, Germany), supplied with a flat plate graphite monochromator, using CuK_α radiation. Phase composition was determined by diffractograms, taken within 2θ values of 5° and 60°.

For a more accurate measurement of the TiO_2 unit cell parameters the diffractograms were taken in the regions of 22°–30° and 46°–52°, using lines (101) and (200) for the anatase structure, and in the regions of 52°–59° and 88°–93°, using lines (222) and (330) for the rutile structure. The rates of counteroperation were equal to 1°/min and $\frac{1}{4}$°/min for the standard and precision measurements, respectively. The size of the coherent scattering region (CSR) was determined from the widening of diffraction lines, using the Selyakov–Sherrer formula.

The electric conductivity method is described elsewhere (31). The support and catalyst powders were crushed, ground, and pressed under 200 bar for 10 min into thin round pellets 0.03 × 0.5 cm in size. The electric conductivity of pelletized samples were investigated in the static cell with voltage of 1 V, temperature of 623 K, and oxygen pressure 0.21 bar, using a B7-26 universal voltmeter. The dc measurements were carried out using a consecutive circuit with both standard (R_o) and metered (R_m) resistance. The resistance of the catalyst pellet was calculated as

$$R_m = R_o U_m (1-U_m)^{-1},$$

where U_m is the drop of voltage across the catalyst pellet.

The main parameters of the pore structure of the TiO_2 and V_2O_5–TiO_2 catalysts were measured in an ASAP-2400 Micromeritics automatic volumetric apparatus, using the low temperature nitrogen adsorption isotherms. The differential curves of mesopore size distribution were calculated from the desorption branches of nitrogen adsorption isotherms, using the method described in (32).

The concentrations of reduced vanadium ions V^{4+} in the oxidized and steady-state catalysts 8.21-A IV and 4.93-R III were measured at 140 K with an ERS-221 EPR spectrometer after dissolving. It is well known that V^{4+} ions in solid samples can become undetectable due to the strong dipole and exchange interactions. Previously we have shown that such samples can be analyzed successfully by EPR after their selective dissolving in 3 *N* H_2SO_4 at 383 K (33). Such treatment did not lead to any change in the vanadium valence state (34, 35).

The total concentration of soluble V^{4+} and V^{5+} ions was measured after similar treatment with a calculated quantity of Mohr's salt in 3 *N* H_2SO_4, using ICP and EPR. The possible influence of 3 *N* H_2SO_4 and Mohr's salt was taken into account. For EPR the concentration of V^{4+} ions was found as a ratio of a sample peak area to the $VOSO_4$ standard solution peak area for the second component of EPR spectrum HFS. The numerical integration of the total spectrum, using $CuCl_2$, $MnCl_2$, and $VOSO_4$ standards, confirmed the possibility of V^{4+} quantitative analysis for the similar spectra.

2.2. *Gases*

Commercial helium, used in this study, was of a special purity grade. The mixture of 5 vol% commercial ammonia with He was dried and purified of organic impurities using columns packed with KOH and charcoal. NO (99.78%)

was prepared by heating the mixture of KNO_2, KNO_3, Cr_2O_3, and Fe_2O_3, as described in (36). The gas mixture of 5 vol% NO in He was cleaned by passing through columns packed with γ-Al_2O_3 and 13X molecular sieves. Commercial nitrous oxide was used without additional purification (1.6 vol% N_2O, balance He). The mixture of 10 vol% O_2 in He was dried on silica gel and 10X molecular sieves.

2.3. Apparatus

The catalytic activity of samples was determined in a flow recycle reactor, with the recycle ratio being 200. All stainless steel lines, six-way pneumatic valves, and a circulating pump were heated to 408 K to preclude salt formation. A glass reactor was placed inside the electrical furnace and supplied with an air flow. The capacity of a specially designed membrane circulating pump was 1000 liters/h at 408 K.

The recently published kinetic data on selective catalytic reduction of NO and V_2O_5–TiO_2 catalysts show that the majority of studies were performed in flow reactors with considerable external diffusion. The excessive catalyst sample weights can serve as the formal criterion for such an estimate. For example, in the well-known work in (37) the conditions of the steady-state experiment were as follows; mixture flow rate, 6 liters/h; concentrations of NO, NH_3, and O_2 of 0.05, 0.05, and 2 vol%, respectively; temperature 523 K; V_2O_5 loading, 1.9 wt%; specific surface, 46 m^2/g; sample weight, 0.1 g. In our experiments under similar conditions the weight of the 2.14-A IV sample was only 0.02 g.

The size of catalyst particles, 0.025–0.05 cm, did not make it possible to avoid a diffusive diminution of reaction rate at 623 and 573 K. Thus, to avoid internal diffusion, the catalysts were pelletized, crushed, and sieved to 0.009–0.016-cm particles. The total sample weight of V_2O_5–TiO_2 catalysts ranged from 0.005 to 0.033 g. Prior to the reaction the catalysts were calcined at 623 K in a flow of 10 vol% O_2/He for 2 h. Then NO, NH_3, and O_2, in a balance of He, were fed. The overall flow rate was 75 cm^3/min. The cycle concentrations of NO, NH_3, and O_2 were 0.17, 0.17, and 2.0 vol%, respectively.

In all experiments a three-column gas chromatograph with an automatic analysis system "Tsvet-500" (Russia) combined with a combustion gas analysis computer "Ecom-Omega" (Austria) permitted the determination of the concentrations of all gases. Chromosorb 104 column with regular sensitivity control and change of the sorbent was used for separating NH_3 and H_2O.

For the analysis of N_2O and NO_2 Porapak QS column can be used. The sensitivity limit for N_2O was 3.0×10^{-3} vol% and permitted the satisfactory estimation of the N_2O concentrations used. Due to the low sensitivity toward NO_2, with threshold equal to 1.57×10^{-2} vol%, the chromatographic method never revealed NO_2 in our reaction mixtures. NO_2 concentrations parallel with NO concentrations were determined with a high accuracy by Ecom-Omega. The gas mixture was diluted 17 times by nitrogen and after NH_3 absorption with concentrated H_3PO_4 was directed to the NO and NO_2 sensors, working within 0–2000 ppm. Inlet NO_2 concentrations, measured by Ecom-Omega, never exceeded 5×10^{-3} vol%. The outlet concentrations were too low to be detected.

N_2/O_2 and NO/N_2 pairs could be analyzed using Molecular Sieves 13X. When the gas mixture contained NO and O_2 at one time, NH_3, H_2O, and NO were preliminarily frozen out at the liquid nitrogen temperature following analysis of N_2 and O_2.

All gas analyses showed the satisfactory material balance according to the equation

$$4\ NO + 4\ NH_3 + O_2 = 4\ N_2 + 6\ H_2O.$$

3. RESULTS

3.1. Catalyst and Support Characteristics

The main characteristics of catalysts, such as vanadia weight loading, support type, specific surface, surface concentration of vanadium atoms, and NO turnover frequencies (TOF), at various temperatures are listed in Table 1. The phase composition of supports and catalysts, the size of coherent scattering region (CSR), cell parameters, specific surface, and electric conductivity of different supports and catalysts are shown in Table 2. For all supports (see Table 2) the grafting of vanadia leads to only a slight decrease of the specific surface area and corresponding increase of CSR size. In contrast, the impregnation method can cause the twofold decrease of surface area from initial value 98 to 44 m^2/g at vanadium monolayer coverage of the catalyst (1).

It can be seen from the microphotographs obtained by scanning electron microscope that A III particles have more branched and loose structure than R III (Fig. 1). Diffractograms of R III and R IV revealed only rutile, and those of A IV only anatase. As for the anatase samples A III, a small admixture of a highly dispersed phase was discovered near $2\theta \approx 30°$. This peculiarity disappeared after vanadia deposition and subsequent heating.

Prepared supports (see Table 2) have unit cell parameters differing from those of ASTM data. This can result for two reasons: high dispersion of TiO_2, which indeed takes place for A IV, A III, and R III samples, and the presence of defects, such as Ti^{3+} ($r\ Ti^{3+} = 0.69$ Å). The latter is quite probable, owing to the method of A III and R III preparation, involving Ti^{3+} compounds.

Parameter "a" for rutile samples R IV and R III is

TABLE 1

Catalyst Characteristics and Activities

Sample	V_2O_5 (wt%)	S_{BET} ($m^2\ g^{-1}$)	$C_V \cdot 10^{-14}$ (atoms V/cm^2)	$TOF_{NO} \cdot 10^3$ (sec^{-1})		
				523 K	573 K	623 K
0.89-A IV	0.89	68	0.87	2.7	9.2	26
2.14-A IV	2.14	108	1.31	4	13	34
4.46-A IV	4.46	110	2.67	5.7	18	52
8.21-A IV	8.21	109	4.97	6.7	24	64
6.60-A IV	6.60	67	6.5	4.3	19	55
3.00-A III	3.00	141	1.92	3.7	7.3	14
(1.30)	(1.30)	141	(0.83)	(8.5)	(16.9)	(32.5)
11.83-A III	11.83	103	7.6	4.4	8.9	20
(5.12)	(5.12)	103	(3.3)	(10)	(20.5)	(47)
0.146-R IV	0.146	9.4	1.04	4.5	13.5	40
1.64-R III	1.64	104	1.04	8	16	31
3.28-R III	3.28	104	2.08	12	23	45
4.93-R III	4.93	103	3.15	13.6	27	52
V_2O_5	100	2	4.86	3.8	11.9	37.7
WO_3		2		0.26	0.81	2
V–W–Ti(I)	3.00	105	2.10[a]	31[a]	52[a]	181[a]
V–W–Ti(II)	3.00	166	1.18[a]	19[a]	43[a]	93[a]

[a] C_V and TOF were calculated, assuming that all vanadium atoms are exposed on the surface.

reduced after vanadia deposition (samples 0.146-R IV and 3.28-R III). This decrease can be explained by the formation of solid solutions of V^{5+} in TiO_2. In this case vanadium atoms are arranged in the flat nets of TiO_2 structure ($r\ Ti^{3+} = 0.64$ Å, $r\ V^{5+} = 0.40$ Å). The similar decrease of the cell parameters is observed for anatase as well after considerable amounts of vanadia are deposited (samples 4.46-A IV and 11.83-A III, Table 2). The introduction of 0.46 wt% of WO_3 into A IV structure increases parameter "a." The simultaneous introduction of vanadia and tung-

TABLE 2

Electric Conductivity (σ) and XRD Data for TiO_2 Supports and V_2O_5/TiO_2 Catalysts

Sample	Phase composition	CSR[a] (Å)	Unit cell parameters (Å)		$\sigma \cdot 10^{10}$ ($\Omega^{-1}\ cm^{-1}$)	S_{BET} (m^2/g)
			a	*c*		
ASTM data[b]	Anatase	>1000	3.7852	9.5139	—	—
A IV	Anatase	105	3.7980	9.5087	10	125
4.46-A IV	Anatase	110	3.7906	9.5087	20	110
A III	Anatase	135	3.7906	9.4873	100	136
3.00-A III	Anatase	150	3.7906	9.4873	150	141
11.83-A III	Anatase	175	3.7869	9.4070	—	103
ASTM data[c]	Rutile	>1000	4.5933	2.9522	—	—
R IV	Rutile	>1000	4.5970	2.9073	—	10
0.146-R IV	Rutile	1000	4.5930	2.9076	—	9.4
R III	Rutile	115	4.6089	2.9672	200	107
3.28-R III	Rutile	115	4.6051	2.9460	450	104
V–W–Ti(I)	Anatase	120	3.791	9.654	1000	105
V–W–Ti(II)	Anatase	80	3.801	9.659	330	166
0.46 WO_3-AIV	Anatase	—	3.794	9.433	—	120

[a] The size of coherent scattering region.
[b] ASTM Card 21-1272.
[c] ASTM Card 21-1276.

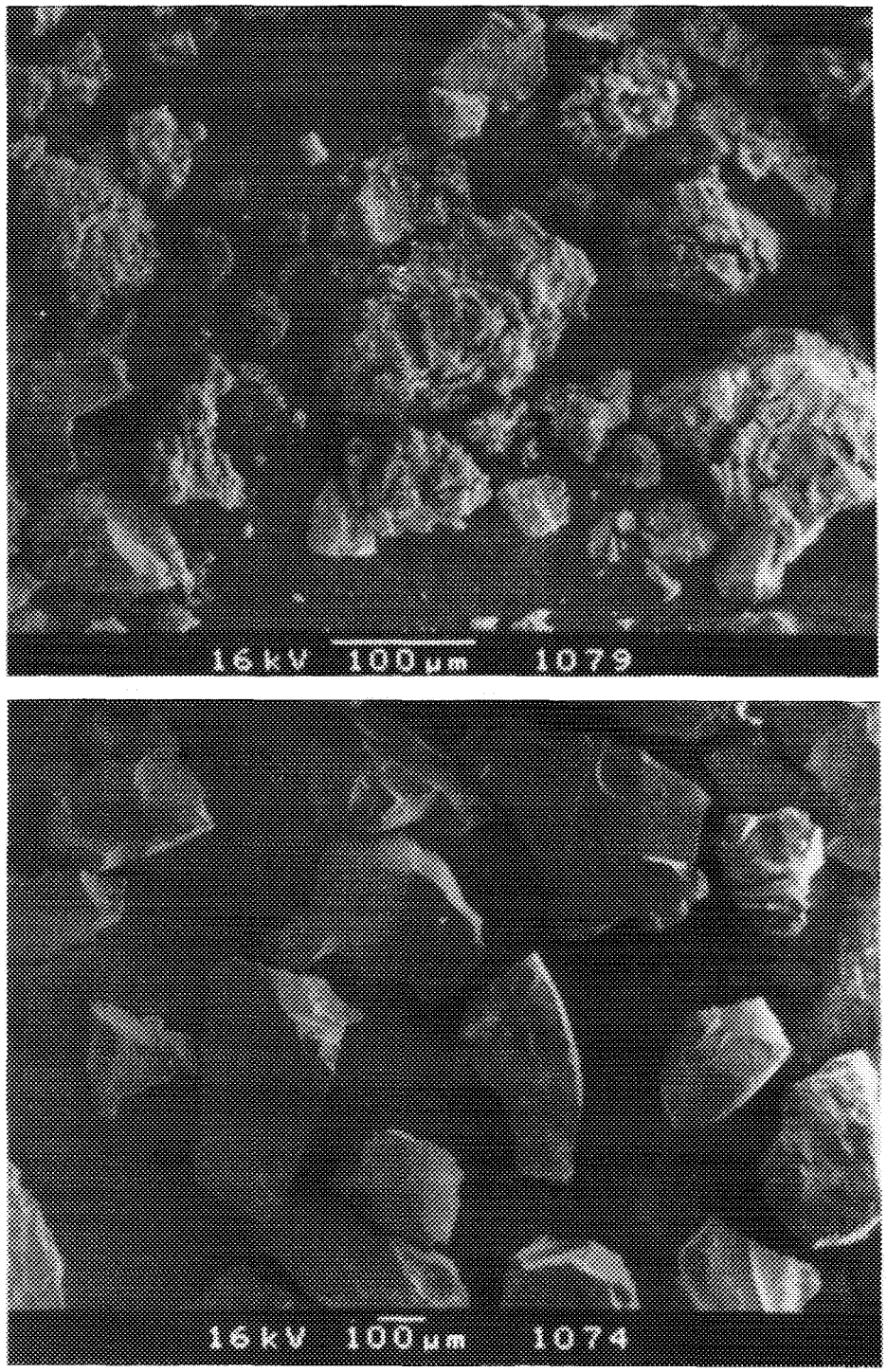

FIG. 1. Morphology of A III (a) and R III (b) samples by scanning electron microscope.

sta into the anatase structure appears to increase both cell parameters (r W^{6+} = 0.65 Å), as can be seen from Table 2.

UV–vis DR spectra of different TiO_2 samples are compared in Fig. 2. Besides the basic absorbance at 45,000–26,000 cm^{-1} typical for the standard rutile and anatase (Fig. 2b), there is a new band at 24,000–20,000 cm^{-1}. Its intensity depends on the preparation method. Moreover, the edge of the basic absorbance for R III sample is shifted to the lower frequencies.

The new absorbance within 24,000–20,000 cm^{-1} could yield from the new shear ordered structures, involving

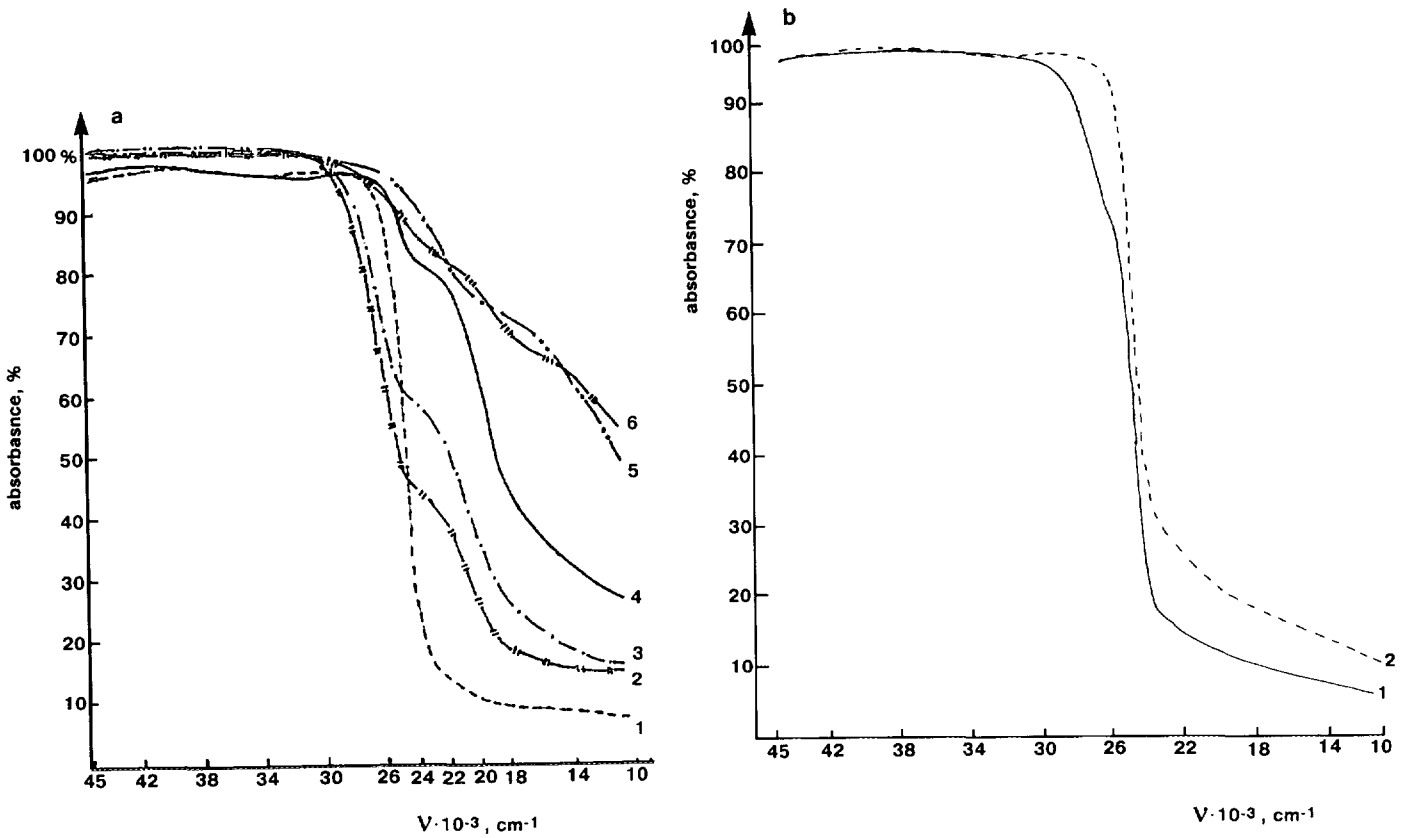

FIG. 2. UV–vis spectra of different titania supports after heating in air at 623 K for 12 h. (a) 1, R IV; 2, A IV; 3, A III; 4, R III; 5, V–W–Ti(I); 6, V–W–Ti(II). (b) For comparison the spectra of anatase, 1, and rutile, 2, standard samples are also shown.

Ti^{3+} ions. This explanation conforms to the high-resolution electron microscopy (HREM) studies of rutile morphology (Fig. 3). Recently the investigation of R III and A III supports and catalysts by HREM has revealed that vanadium atoms react chemically with the titania to form

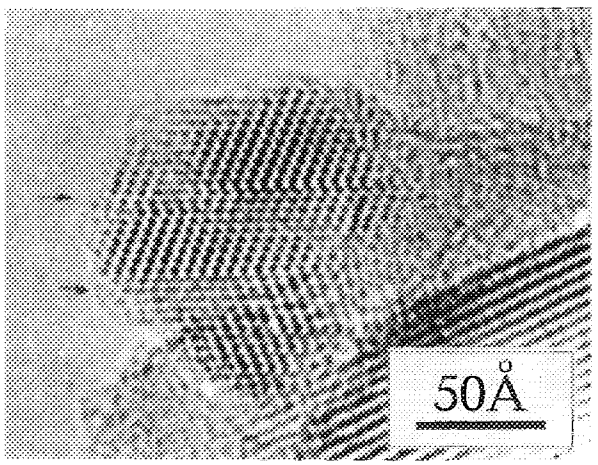

FIG. 3. HREM photograph of rutile R III nanoparticles.

$VTiO_4$ slabs coherently intergrown with rutile. They appear as a pair of closely spaced (100) crystallographic shear planes (38).

The direct measurement of Ti^{3+} concentrations in A IV, A III, and R III samples by EPR method using solid samples at 293 K and 123 K registered no isolated Ti^{3+} ions. As far as samples A IV, A III, and R III have approximately equal surfaces and dispersities, they can possess the similar dissipation characteristics. Thus we can assume the relative absorbance intensity to depend on the defect concentration only. The concentration of defects varies in the following series: A IV < AIII < R III, while for R IV the concentration of defects is negligible.

Simultaneously with the increase of the 24,000–20,000 cm^{-1} band intensity, the absorbance in the region of 18,000–11,000 cm^{-1} also augments, probably due to the increase in the concentration of free charge carriers intensively absorbing the light. This agrees well with the distinct increase of electric conductivity of supports in the series A IV $\ll$ A III < R III (see Table 2). Note that the complex V–W–Ti catalysts have another type of defects (Fig. 2b).

After vanadia grafting the increase of electric conduc-

tivity in oxygen was observed for each pair catalyst/support. This is similar to the results, obtained in (14), where rutile was impregnated with 1 and 8 wt% of vanadia. The increase of electric conductivity seems to result from dissolving of some vanadia in the lattice of titania. Thus heterovalent V^{5+} ions replace Ti^{4+} and form a solid solution in TiO_2. At the same time analysis of electric conductivity in (14) shows that the formation of V_2O_5–TiO_2 systems can be accompanied by formation of highly labile anionic vacancies.

Catalysts of different series 4.46-A IV, 4.93-R III, and 3.00-A III with similar specific surfaces and vanadia weight loadings were found to have no micropores. All samples were monodisperse, the average pore diameters were 159, 71, and 98 Å, and pore volumes were 0.48, 0.19, and 0.33 cm^3/g, respectively. For catalyst 4.93-R III with minimal pore diameter at the highest temperature of experiment 623 K the diffusion efficiency η was calculated. The calculation procedures are described in (39). The diffusion coefficients were taken from (40). The efficiency factor was proved to be 0.99, confirming the absence of internal diffusion effects in our experiment.

The concentration of a soluble fraction of V^{4+} and V^{5+} (A IV, R IV, R III series) was determined with ICP and EPR, after the crushed sample was dissolved in the mixture of Mohr's salt and 3 N H_2SO_4. The soluble fraction is only 70% of the vanadium loading. For various V–Ti catalysts a portion of titanium appeared in solution during this treatment according to ICP method. The number of titanium atoms in solution was approximately the same as the number of vanadium atoms, which remained intact. It should be pointed that the total loading of vanadium was determined by ICP in the separate analysis after the complete sample dissolving.

According to (14), the same portion of vanadium (30%) resisted etching in *i*-butanol, keeping back the concentration of deposited on rutile V_2O_5 bulk phase. The explanation of this phenomenon by the penetration of V^{5+} ions into subsurface layers of titania (14) agrees well with our own data.

For A III series, similar treatment with a mixture of 3 N H_2SO_4 and Mohr's salt showed only 30% of total quantity of grafted vanadium to be soluble (values in parentheses, Table 1). The more efficient penetration of vanadia in this case can occur due to its interaction with a highly dispersed phase, observed in A III samples before their grafting. Only the soluble part of vanadia disposed in the surface layer was used for calculations of the turnover number. Hence with well crystallized TiO_2 supports 30% of supported vanadia can penetrate in the subsurface layers after the grafting and subsequent thermal treatment. In a support, containing a highly dispersed phase, the part of such subsurface vanadia can reach 70% of the total vanadia quantity.

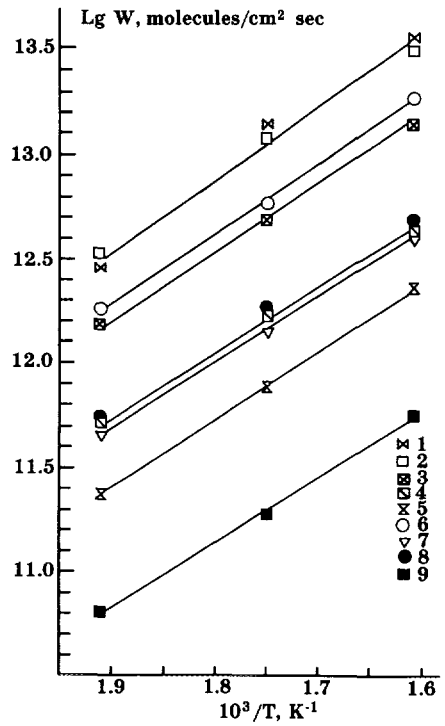

FIG. 4. Comparison of the Arrhenius plots for NO selective reduction steady-state specific rates on V_2O_5 and V_2O_5–TiO_2 catalysts, supported on A IV and R IV. NO, NH_3, O_2 cycle concentrations are equal to 0.17, 0.17, and 2.0 vol%, respectively. Open symbols, with oxygen; closed symbols, without oxygen. 1, 6.60-A IV; 2, 8.21-A IV; 3, 4.46-A IV; 4, 2.14-A IV; 5, 0.89-A IV; 6, V_2O_5; 7, 0.146-R IV; 8, V_2O_5; 9, 4.46-A IV.

According to the XRD method the phase structure of unsupported V_2O_5 did not change after NO–NH_3–O_2 feeding, but after NO–NH_3 feeding the unloaded catalyst represented V_2O_4 phase, completely soluble in 3 N H_2SO_4. The concentration of V^{4+} ions in the supported catalysts 8.21-A IV and 4.93-R III before and after NO–NH_3–O_2 feeding proved to be 40% from the total amount of V atoms.

The time of steady state establishment in NO–NH_3–O_2 experiments did not exceed the duration of a single chromatographic analysis. It is well known that the oxygen of vanadia can participate in the NO–NH_3 reaction in the absence of gaseous oxygen (25). Without oxygen the time required to establish a steady state at 623 K was 1 h for supported 4.46-A IV and 10 h for unsupported V_2O_5.

3.2. *Catalytic Activity and Selectivity*

Figure 4 shows the Arrhenius plots of NO SCR within 523 K and 623 K for V_2O_5–TiO_2 catalysts, supported on A IV and R IV. Evidently, the specific activity of this group of catalysts increases with the vanadia weight loading. All activation energies of SCR for V_2O_5, unsupported

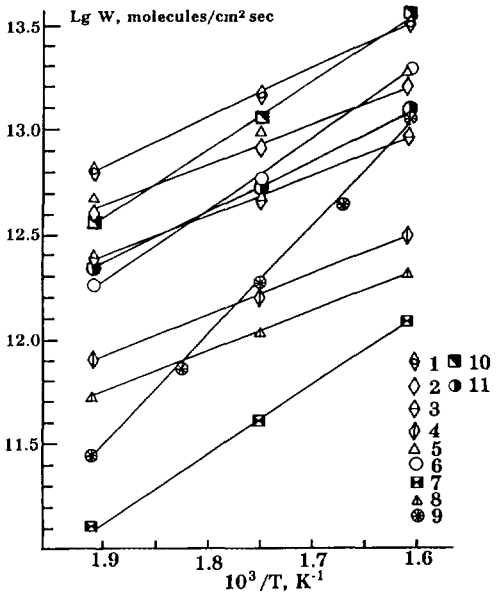

FIG. 5. Comparison of Arrhenius plots for NO selective reduction (1–8) and NH_3 oxidation with O_2 (9) steady-state specific rates on V_2O_5, WO_3, $V_2O_5/WO_3/TiO_2$ and V_2O_5/TiO_2 catalysts, supported on R III and A III. NO, NH_3, O_2 cycle concentrations are 0.17, 0.17, 2.0 vol%, respectively. In parentheses, concentrations of the soluble part of vanadia supported on A III. 1, BASF-0481; 2, 4.93-R III; 3, 3.28-R III; 4, 1.64-R III; 5, 11.83(5.12)-A II; 6, V_2O_5; 7, WO_3, 8, 3.00(1.30)-A III; 9, V_2O_5; 10, V-W-Ti(I); 11, V-W-Ti(II).

and supported on anatase or rutile, if prepared from Ti^{4+} compounds, are equal to 14–15 kcal/mol and are practically constant within the error limits.

Note that the activation energies for NO catalytic reduction with NH_3 without oxygen coincide with their values in the presence of oxygen both for unsupported V_2O_5 and 4.46-A IV. The specific rate of NO catalytic reduction without oxygen was threefold lower for unsupported V_2O_5 and 23 times lower for 4.46-A IV than the rate in the presence of O_2.

Figure 5 shows the Arrhenius dependence for another group of vanadia catalysts supported on anatase or rutile and prepared using Ti^{3+} compounds. The growth of the R III series specific activity with vanadia weight loading is evident. Unexpectedly, the specific activities of A III catalysts proved to be far lower than those of R III catalysts (at almost the same vanadia weight loading). The SCR activation energies for A III and R III catalysts are significantly lower than those of A IV and R IV series, reaching only 9–10 kcal/mol, and are practically constant within the error limits.

The activation energy determined on industrial catalyst BASF-0481 (10.7 kcal/mol) shows the addition of WO_3 to the V_2O_2–TiO_2 to affect the system in the same way as Ti^{3+} does. Note that SCR activation energies for the individual components of this industrial catalyst, such as V_2O_5, WO_3, and for V_2O_5/A IV, are equal to 15 kcal/mol (see Fig. 5).

The same figure permits the comparison of the specific activity of unsupported vanadia in SCR and in NH_3 oxidation with oxygen (SCO). For the cycle concentration of NH_3, equal to 0.17 vol%, the SCR rate is six times higher at 523 K and only 1.7 times higher at 623 K than the SCO rate. The activation energy for NH_3 oxidation was found to be 24 kcal/mol.

Figure 6 shows a plot of SCR steady-state specific rates versus vanadium surface concentrations for A IV and R III series of supported catalysts. Obviously, in spite of the different nature of supports used, the specific activity of R III series coincides at 623 K with that of A IV series. At the lower temperatures the specific activity of R III series proved to be only insignificantly higher than the activity of A IV series. The order of SCR-specific rate dependence on vanadium surface concentration, found from the incline of plots of log W versus log C_v, was equal to 1.6–1.7.

Table 1 lists the values of TOF (molecules of NO/atoms of V s) for various catalysts used at various temperatures. The values of vanadia monolayer capacity, recently estimated for V_2O_5–TiO_2 catalysts, range in different works from 8.7 (9) and 7.9 (11) to 6.86 (12) and 5 nm^{-2} in (10). We accepted in our work as the most reliable the capacity found recently by XPS by Andersson (12) and equal to

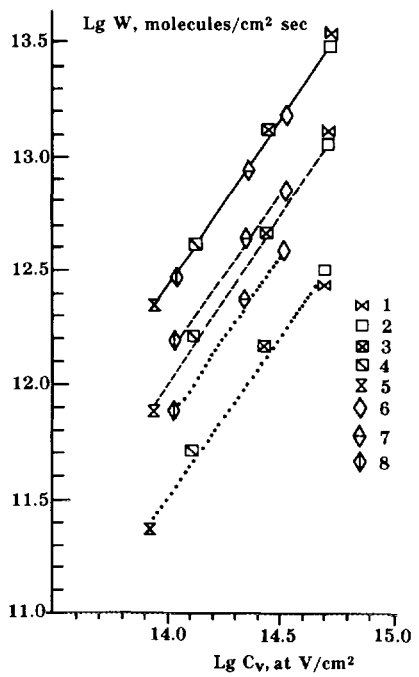

FIG. 6. A plot of SCR-reaction steady-state specific rate versus vanadium atom concentration. 1, 6.60-A IV; 2, 8.21-A IV; 3, 4.46-A IV; 4, 2.14-A IV; 5, 0.89-A IV; 6, 4.93-R III; 7, 3.28-R III, 8, 1.64-R III. Solid line, 623 K; dashed lines, 573 K; dotted lines, 523 K.

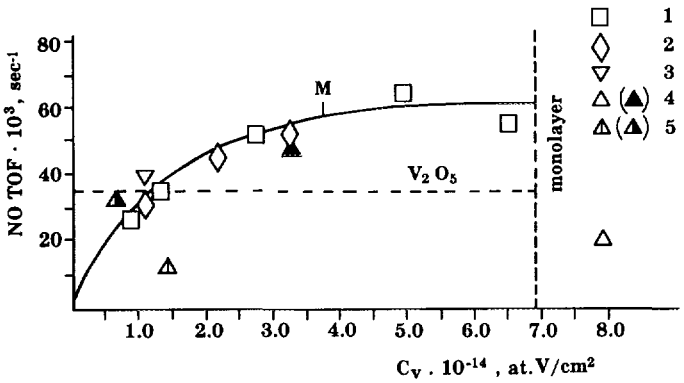

FIG. 7. The turnover frequency for NO reduction of 623 K versus vanadium atoms concentration for V_2O_5–TiO_2 samples. Data are shown for NO, NH_3, O_2 cycle concentrations of 0.17, 0.17, 2.0 vol%, respectively. 1, Catalysts of A IV series; 2, catalysts of R III series; 3, 0.146-R IV; 4, 11.83-A III; 5, 3.00-A III. 4,5. (In parentheses) the concentration of the soluble part of supported vanadia. Closed symbols, TOF, calculated using the concentration of V atoms in the soluble part of supported vanadia. M, the smallest surface concentration of V atoms in (2).

6.86 nm^{-2}. The concentration of V=O species on the surface of unsupported V_2O_5, used in our calculations, was equal to the surface density of V=O groups on the (010) face, 4.87 nm^{-2}, in agreement with (41, 42).

The turnover frequencies for NO reduction at 623 K versus vanadium atom concentration for different V_2O_5–TiO_2 and V_2O_5 samples are shown in Fig. 7. These data show that the wide variation of vanadia surface concentration leads only to the twofold increase of NO turnover number. At 623 K there is no difference in turnover numbers for different supports except for A III samples.

For the latter samples the atomic activity related to the total amount of vanadium in the sample was proved to be much lower (see Fig. 7). If the turnover numbers for A III series are calculated only for the soluble portion of vanadium (shown in the parentheses of Fig. 7), the values obtained (designated by closed symbols) fit the curve obtained satisfactorily.

The average value of TOF for the monolayer coverage of supports with V atoms proved to be 6×10^{-2} s^{-1} at 623 K, while TOF for the unsupported V_2O_5 was equal to 3.7×10^{-2} s at the accepted V atom monolayer capacity. The TOF value calculated from data of Bell *et al.* (1) on anatase supported vanadia under conditions comparable with our own (523 K, NO and NH_3 concentrations of 0.17 vol%) for an activation energy of 15 kcal/mol and for the first reaction order toward NO was 3.3×10^{-3} s. This value is slightly lower in comparison to the average TOF 5×10^{-3} s at 523 K determined in this paper. This can be explained by the influence of either a higher oxygen pressure in our experiment (2 vol%) or internal diffusion in the catalyst particles 0.06–0.03 cm in size used in (1).

The supported catalysts in (1) were prepared by incipient wetness impregnation with vanadium oxalate solution. According to the Raman spectra of freshly oxidized samples near vanadium monolayer concentrations, their surface contains 50% of the monomeric species and 50% of the 10 times more active polyvanadate species. Unlike these catalysts, the surface of the grafted V_2O_5–TiO_2 samples, as shown by high-resolution NMR studies (43), within vanadium monolayer concentrations is covered only by tetrahedral vanadium species of two types with a nearly regular structure. This permits us, when we calculate the NO turnover numbers, to relate the activity to the overall quantity of V=O groups on the surface.

The structure-insensitivity of the NO–NH_3–O_2 reaction was first demonstrated by Murakami *et al.* (2) for the impregnated anatase-supported vanadia catalysts, washed from the bulk vanadia by ammonium hydroxide. The turnover numbers for V_2O_5, supported and unsupported, in relation to the surface V=O concentrations and determined by the method of rectangular impulses were shown to be equal. The maximal V=O concentration in the monolayer established by this method was only 2.76 nm^{-2}, while the overall vanadium atom monolayer concentration, according to (12), was 6.86 nm^{-2}. The calculation of TOF for 523 K, using the E_a value of 11 kcal/mol (2) and the total surface vanadium concentration near the monolayer, gives 5.7×10^{-3} s^{-1}, which is in line with our data.

As for reaction selectivity, at 523–623 K no nitrous oxide was observed for any V_2O_5–TiO_2 catalysts in NO–NH_3 and NO–NH_3–O_2 experiments or for V_2O_5 in NO–NH_3–O_2 and NH_3–O_2 experiments. The outlet concentrations of N_2O for NO–NH_3 interaction on V_2O_5 at 573 and 623 K and for NO–NH_3–O_2 interaction on WO_3 at 623 K correspond to the N_2O selectivity, defined as $[N_2O]/([N_2] + [N_2O])$ and equal to 15 and 17%, respectively.

Direct N_2O interaction with NH_3 at 0.17 vol% cycle concentrations of both gases between 523 K and 623 K in the presence of 2 vol% of oxygen and without it on the catalyst 8.21-A IV revealed no reduction of N_2O to N_2. Only ordinary NH_3 oxidation was observed. So the mechanism of NO–NH_3–O_2 reaction postulated in (44), with absorbed N_2O as the main intermediate, can hardly be adopted.

4. DISCUSSION

1. We intended to obtain the reliable kinetic data and turnover frequencies in NO–NH_3–O_2 reaction for vanadia monolayer catalysts on titania support (rutile and anatase). One of the main results is the coincidence of specific activities and activation energies for vanadia grafted on rutile R IV and anatase A IV. Unsupported vanadia has

the same activation energy and twofold lower specific activity. The turnover frequencies for these two series of catalysts, A IV and R IV, also coincide. The turnover frequency of unsupported vanadia is twofold lower than that of supported vanadia.

Thus, the chemical nature of titania is responsible for the high activity of vanadia–titania catalysts in SCR. The particular role of the anatase crystal structure, deduced from the fit of the (010) V_2O_5 plane and the (001) anatase plane in (28), is not confirmed by our kinetic data.

2. Neglecting the insignificant differences in specific activity and turnover frequency for supported and unsupported vanadia, we can assume the mechanism of SCR to be common for these systems. The observed difference in turnover frequencies and specific activities can be explained by some uncontrolled impurity in the extra pure vanadia with the low surface area of 2 m^2/g, which can be concentrated on the surface, or by another fine surface effect, e.g., the promoting effect of titania.

3. According to (43), the surface of titania-supported vanadia, obtained by grafting within monolayer concentrations, is covered by tetrahedral vanadium species of two types with a nearly regular structure. The turnover frequencies, in relation to the surface concentration of vanadium atoms, increase only twice within a wide range of vanadia surface concentration. The twofold increase may result from the easier reoxidation of reduced surface vanadium ions by oxygen with increased surface V concentration and, thus, with increased probability of adjacent vacancies forming.

4. NO reduction by ammonia with gaseous oxygen (SCR) and without it shows the same activation energy (15 kcal/mol) for both unsupported and supported vanadia. The period of steady-state establishment in the reaction without oxygen is long, and according to the material balance and XRD data the process is accompanied by vanadia reduction to V_2O_4. Without oxygen the preexponential factor for unsupported vanadia becomes 3-fold lower, while for the supported sample a 23-fold decrease is observed. The data obtained can be explained by the common mechanism of both $NO–NH_3–O_2$ and $NO–NH_3$ reactions at the different surface concentrations of V=O species. In the case of SCR the reoxidation of oxygen vacancies by the gaseous oxygen may be an additional reaction step.

Reoxidation by NO would have the lower rate, for it needs two adjacent oxygen vacancies, while O_2 adsorption can proceed on a single oxygen vacancy with subsequent O_2 dissociation and migration to the neighbor vacancy. The far smaller decrease of the NO specific reduction rate without oxygen for the unsupported vanadia can be explained by the role of its bulk in the transfer of anion vacancies.

5. The order of specific rate dependence on vanadium surface concentration for SCR on A IV series catalysts, found from the incline of plots of log W versus log C, is equal to 1.6–1.7. This finding is consistent with the observed increase of turnover frequency for the same range of vanadium surface concentrations $<5 \times 10^{14}$ atoms of V/cm^2 (see point 2).

The assumption of second-order specific rate dependence on V surface concentration is in agreement with the SCR mechanism, advanced in (18), where two V atoms are needed for the conversion of one NO (NH_3) molecule. It should be stressed nonetheless that the real relationship between the specific rate and the V concentration, as well as between V pair concentration and coverage, can be more complicated and needs further analysis.

6. Catalysts composed of one or several of the *n*-type semiconductor oxides (e.g., V_2O_5, TiO_2, WO_3) are known for a higher activity in $NO–NH_3–O_2$ reaction than those containing *p*-type semiconductor oxides. This is attributed to the ability of *n*-type semiconductor oxides to retain anion vacancies, thus favoring NO and O_2 adsorption (45). By varying the semiconductor properties of titania we can elucidate both the mechanism of its promoting effect and the mechanism of the SCR process.

There are two common methods of changing the electric conductivity of titania. The first method involves the preparation of oxide with nonstoichiometric composition, inserting interstitial Ti^{3+} ions by annealing at 1073–1373 K (46). It is obvious that the samples obtained by this method will always possess a rutile structure with a small surface area. In our work the insertion of Ti^{3+} ions into the anatase (A III) and rutile (R III) structures with high dispersion was realized by preparation of titania from Ti^{3+} compounds. It is known that the deviations from stoichiometry and the possible electric conductivity changes for such samples are not large.

The electric conductivity σ of rutile, annealed in oxygen at 1223 K, is equal to $10^{-10}\ \Omega^{-1}\ cm^{-1}$. The sample of anatase A IV contains some defects, which are easily annealed at 723 K, and has electric conductivity σ in oxygen equal to $10^{-9}\ \Omega^{-1}\ cm^{-1}$. Chemical insertion of Ti^{3+} ions generates defects stable at temperatures higher than 1073 K, with σ (for A III and R III samples) equal to 1×10^{-8} and $2 \times 10^{-8}\ \Omega\ cm^{-1}$, respectively.

Unlike the catalysts of the A IV and R IV series, vanadia catalysts grafted onto A III and R III supports exhibit appreciably lower activation energies (9–10 kcal/mol) in SCR. Specific rates and turnover frequencies, in relation to the surface concentration of vanadium atoms, remain nearly equal to those found for vanadia grafted on A IV and R IV.

The enhancement of the *n*-type conductivity of titania via insertion of Ti^{3+} impurities can facilitate the transfer of anion vacancies. The appreciable decrease of activation energy for SCR reaction in this case can mean that the

key step of the process relates to the charge transfer in the subsurface layers of catalyst particles.

7. The second method allowing the preparation of stable and homogeneous semiconductors with a large range of electric conductivity is based on the "valence induction" phenomena discovered by Verway. Insertion of cations with different valences, e.g., W^{6+}, into TiO_2 is compensated by the appearance of equivalent amounts of Ti^{3+} cations.

Tungsta addition to titania (rutile) is known to enhance both the electric conductivity and the oxygen chemisorption rate with simultaneous diminution of electric conductivity activation energy (47). UV–vis spectra of V_2O_5–WO_3–TiO_2 samples reveal additional specific absorbance within 24,000 and 20,000 cm^{-1}, more intensive than the absorbance of A III and R III samples in this region.

Thus, it is quite reasonable to assume that tungsta addition to titania-supported vanadia accelerates the reoxidation of oxygen vacancies $V_{\blacksquare}$. NO reduction without oxygen and reduction of supported vanadia catalysts during SCR reaction convincingly show that SCR is hindered by reoxidation of vanadium.

Obviously, tungsta addition to titania and vanadia in the case of complex V–W–Ti catalysts not only creates a higher concentration of defects, according to UV–vis data, and augments the electric conductivity in oxygen up to $10^{-7}\ \Omega^{-1}\ cm^{-1}$, but can also in some cases diminish the activation energy of SCR process to 10.6 kcal/mol, resulting in a nonadditive increase of specific activity in SCR. The decrease of activation energy can be connected tentatively with the V^{4+} fraction in the total vanadium content. For the complex catalyst V–W–Ti(I) with a higher activation energy, 15 kcal/mol, the V^{4+} content was threefold less than for V–W–Ti(II), which contained 40% of V^{4+}.

8. Irrespective of the method of vanadia introduction (impregnation, grafting) and of the crystal structure of titania, the etching of V_2O_5–TiO_2 catalysts by a mixture of 3 N_2SO_4 and Mohr's salt reveals only a partial dissolving of vanadia (usually 70%). The rest of vanadia, which resists etching, penetrates into the deeper sublayers of titania, and heterovalent V^{5+} ions replace Ti^{4+} ions. The equivalent of the amount of titanium ions substituted appears in the solution during the etching.

CONCLUSIONS

On the basis of data presented above concerning kinetic studies as well as physical and chemical characteristics of grafted titania-supported vanadia catalysts, we can draw the following conclusions:

1. The specific activity, activation energy, and turnover frequency do not depend substantially on the crystal structure of titania.

2. The SCR reaction on titania-supported vanadia hardly depends on the concentration of vanadium atoms.

3. The activation energy of the SCR process nearly coincides with the vanadia reoxidation activation energy estimated in our earlier studies (15 and 16 kcal/mol, respectively) (48). Reoxidation of reduced vanadia species (V–OH, $V_{\blacksquare}$) seems to be the rate-limiting step of the SCR process.

4. Reduction of nitrogen oxide by ammonia with and without oxygen may have a common reaction mechanism with peculiar steps involving reoxidation by gaseous oxygen and nitrogen oxide and different surface V=O concentrations.

5. Conversion of one NO (NH_3) molecule apparently proceeds on two surface vanadium atoms.

6. Independent of the method of vanadia introduction and the titania crystal structure a part of supported vanadia (commonly 30%) penetrates into the sublayers of titania. V^{5+} ions replace Ti^{4+} ions. An amount of titanium ions equivalent to those displaced can be washed out from the surface selectively.

7. Titania modified by Ti^{3+} and W^{6+} ions assumes an ordered shear structure with enhanced electric conductivity and oxygen adsorption rate (49).

8. Regulation of *n*-semiconductor properties of the titania support via insertion of Ti^{3+} and W^{6+} ions is a powerful tool for modification of catalytic activity of vanadia catalysts in the SCR process.

ACKNOWLEDGMENTS

The authors thank A. F. Bedilo, V. K. Ermolaev for EPR measurements, N. N. Boldyreva, I. L. Kraevskaya for chemical analysis of catalysts, A. V. Kalinkin for XPS analysis of supports, A. A. Rar for SIMS measurements, and V. F. Anufrienko for useful discussions.

REFERENCES

1. Went, G. T., Leu, L.-J., Rosin, R. R., and Bell, A. T., *J. Catal.* **134,** 492 (1992).
2. Murakami, Y., Inomata, M., Miyamoto, A., and Mori, K., "Proceedings, 7th International Congress on Catalysis, Tokyo, 1980" (T. Seiyama and K. Tanabe, Eds.). Elsevier, Amsterdam, 1981.
3. Ramis, G., Busca, G., Bregani, F., and Forzatti, P., *Appl. Catal.* **64,** 258 (1990).
4. Dines, T. J., Rochester, C. H., and Word, A. M., *J. Chem. Soc. Faraday Trans.* **87,** N 9, (1991).
5. Nam, I.-S., *J. Catal.* **119,** 269 (1989).
6. Duffy, B. L., Curry-Hyde, H. E., Cant, N. W., and Nelson, P. F., *J. Phys. Chem.* **97,** 1729 (1993).
7. Tufano, V., and Turco, M., *Appl. Catal. B* **2,** 9 (1993).
8. Srnak, T. Z., Dumesic, J. A., Clausen, B. S., Tornqvist, E., and Topsoe, N.-Y., *J. Catal.* **135,** 246 (1992).
9. Bond, G. C., and Tahir, S. F., *Appl. Catal.* **71,** 1 (1991).
10. Pinaeva, L. G., Rar, A. A., Kalinkin, A. V., Zaikovskii, V. I.,

Ivanov, A. A., Balzhinimaev, B. S., *React. Kinet. Catal. Lett.* **41,** 375 (1990).
11. Machej, T., Haber, F., Turek, A. M., and Wachs, I. E., *Appl. Catal.* **70,** 115 (1991).
12. Lars, S., and Andersson, T., *Catal. Lett.* **7,** 351 (1990).
13. Wong, W. C., and Nobe, K., *Ind. Eng. Chem. Prod. Res. Dev.* **23,** 564 (1984).
14. Herrmann, J. M., and Disdier, J., *EUROPACAT-1*, Montpellier, September 12–17, 1993. [Book of Abstracts, Vol. 2, 978]
15. Miyamoto, A., Kobayashi, K., Inomata, M., and Murakami, Y., *J. Phys. Chem.* **86,** 2945 (1982).
16. Miyamoto, A., Yamazaki, Y., Inomata, M., and Murakami, Y., *J. Phys. Chem.* **85,** 2366 (1981).
17. Topsoe, N.-Y., *J. Catal.* **128,** 499 (1991).
18. Janssen, F. J. J. G., van der Kerkhof, F. M. G., Bosch, H., Ross, J. H. R., *J. Phys. Chem.* **91,** 521 (1987).
19. Farber, M., and Harris, S. P., *J. Phys. Chem.* **88,** 680 (1984).
20. Dines, T. J., Rochester, S. H., and Ward, A. M., *J. Chem. Soc. Faraday Trans.* **87** (10), 1611 (1991).
21. de Boer, M., Huisman, H. M., Mos, R. J. M., Leliveld, R. G., van Dillen, A. J., and Geus, J. W., *Catal. Today* **17,** 189 (1993).
22. Bjorklund, R. B., Odenbrand, C. U. I., Brandin, J. G. M., Andersson, L. A. H., Liedberg, B., *J. Catal.* **119,** 189 (1989).
23. Ozkan, U. S., Cai, Y., and Kumthekar, M. W., *Appl. Catal. A* **96,** 365 (1993).
24. Bosch H., Janssen, F., *Catal. Today* **2,** 369 (1987).
25. Inomata, M., Miyamoto, A., and Murakami, Y., *Chem. Lett.* 799 (1978).
26. Inomata, M., Miyamoto, A., and Murakami, Y., *J. Catal.* **62,** 140 (1980).
27. Odenbrand, I., Lundin S., and Andersson, L., *Appl. Catal.* **18,** 335, (1985).
28. Vejux, A., and Courtine, P., *J. Solid State Chem.* **23,** 93 (1978).
29. Cai, Y., and Ozkan, U. S., *Appl. Catal.* **78,** 241 (1991).
30. Bond, G. C., and Konig, P., *J. Catal.* **77,** 309 (1978).
31. Ponomareva, V. G., and Khairetdinov, E. F., *Izvestiya SO AN*, Seriya Khim. Nauk **8,** 27 (1985). [in Russian]
32. Broekhoff, J. S. P., and de Boer, J. N., *J. Catal.* **9,** 8 (1967).
33. Marshneva, V. I., Boreskov, G. K., and Sokolovskii, V. D., First Soviet-Japanese Seminar on Catalysis, July 1971, Novosibirsk, USSR, Preprint 25.
34. Elizarova, G. L., and Kuznetsova, A. S., *Zh. Anal. Khim.* **33,** 50 (1968).
35. Cavani, F., and Trifiro, F., *Catal. Today* **2,** 369 (1989).
36. Ray, J. D., and Ogg, R. A., Jr., *J. Am. Chem. Soc.* **78,** 5993 (1956).
37. Bosch, H., Janssen, F., van Kerkhof, T., Oldenziel, J., van Ommen, J., and Ross, J., *Appl. Catal.* **25,** 239 (1986).
38. Kryukova, G. N., and Kalinkina, O. V., in "Proceedings Spring MRS Meeting, San Francisco, 1994." p. 129.
39. Malinovskaya, O. A., Beskov, V. S., and Slinko, M. G., Modelirovanie Katalyticheskikh Processov na Poristyikh Zernakh [The Simulation of Catalytic Processes on Porous Particles], Novosibirsk, Nauka, 1975, p. 266. [in Russian]
40. Vargaftik, N. B., Ed., "The Reference Book for Thermophysical Properties of Gases and Liquids," Nauka, Moscow, 1972. [in Russian]
41. Andersson, A. *J. Solid State Chem.* **42,** 3 (1982).
42. Inomata, M., Miyamoto, A., and Murakami, Y., *J. Chem. Soc. Chem. Commun.* **21,** 1009 (1979).
43. Pinaeva, L. G., Lapina, O. B., Mastikhin, V. M., Nosov, A. N., and Balzhinimaev, B. S., *J. Mol. Catal.* **88,** 311 (1994).
44. Marangozis, J., *Ind. Eng. Chem. Res.* **31,** 987 (1992).
45. Matsuda, S., and Kato, A., *Appl. Catal.* **8,** 149 (1983).
46. Gautron J., Marucco, J. F., and Lemasson, P., *Mat. Res. Bull.* **16,** 575 (1981).
47. Mikhailova, I. L., Candidate Thesis, Institute of Catalysis, Novosibirsk (1968).
48. Marshneva, V. I., Boreskov, G. K., and Sokolovskii, V. D., *Kinet. i Katal.* **13** (N2), 393–398 (1972).
49. Blanchin, M. G., Bursill, L. A., and Smith, D. J., *Proc. R. Soc. London A* **391,** 351–372 (1984).